

DETECTION OF THE ISW AND SZ EFFECTS FROM THE CMB-GALAXY CORRELATION

PABLO FOSALBA¹, ENRIQUE GAZTAÑAGA^{2,3}, FRANCISCO J CASTANDER²*Accepted by ApJLett*

ABSTRACT

We present a cross-correlation analysis of the WMAP cosmic microwave background (CMB) temperature anisotropies and the SDSS galaxy density fluctuations. We find significant detections of the angular CMB-galaxy correlation for both a flux limited galaxy sample ($z \sim 0.3$) and a high redshift ($z \sim 0.5$) color selected sample. The signal is compatible with that expected from the integrated Sachs-Wolfe (ISW) effect at large angles ($\theta > 4^\circ$) and the Sunyaev-Zeldovich (SZ) effect at small scales ($\theta < 1^\circ$). The detected correlation at low- z is in good agreement with a previous analysis using the APM survey ($z \sim 0.15$). The combined analysis of all 3 samples yields a total significance better than 3σ for the ISW and about 2.7σ for the SZ, with a Compton parameter $\bar{y} \simeq 10^{-6}$. For a given flat Λ CDM model, the ISW effect depends both on the value of Ω_Λ and the galaxy bias b . To break this degeneracy, we estimate the bias using the ratio between the galaxy and mass auto-correlation functions in each sample. With our bias estimation, all samples consistently favor a best fit dark-energy dominated model: $\Omega_\Lambda \simeq 0.8$, with a 2σ error $\Omega_\Lambda = 0.69 - 0.86$.

Subject headings: cosmic microwave background, cosmology: observations

1. INTRODUCTION

A recent study (Fosalba & Gaztañaga 2003) has cross-correlated the cosmic microwave background (CMB) anisotropies measured by WMAP (Bennett et al. 2003) with galaxy fluctuations in the APM Galaxy Survey (Maddox, Efstathiou, Sutherland, & Loveday 1990) to find significant detections for both the integrated Sachs-Wolfe (ISW) and thermal Sunyaev-Zeldovich (SZ) effects. The ISW detection is in agreement with other analyses based on X-ray and radio sources (Boughn & Crittenden 2003; Nolta et al. 2003), while Hernandez-Monteagudo & Rubino-Martinez (2003) fail to detect the SZ effect when comparing WMAP to different cluster templates (see also Myers et al. (2003)). It should be stressed nevertheless that cluster or galaxy group catalogues are too sparse and typically produce worse signal-to-noise ratios than galaxy surveys. Moreover, depending on the sample there could be a significant cancellation of the ISW and SZ effects on scales smaller than a few degrees (see §4). In this letter we cross-correlate the WMAP CMB temperature anisotropies with galaxies from the Sloan Digital Sky Survey (SDSS; York et al. 2000). When we were finishing this work we became aware of a similar analysis (Scranton et al. 2003) that uses different color and photometric redshift selected samples from the SDSS.

2. DATA

We make use of the largest datasets currently available to study the CMB-galaxy cross-correlation. In order to probe the galaxy distribution, we have selected subsamples from the SDSS Data Release 1 (SDSS DR1; Abazajian et al. 2003) which covers ~ 2000 deg 2 (i.e. 5 % of the sky). The samples analyzed here have different redshift distributions and a large number of galaxies

(10^5 - 10^6 , depending on the sample). We concentrate our analysis on the North sky (~ 1500 deg 2 , ie, 3.6 % of the sky), because it contains the largest and wider strips. The South SDSS DR1 (~ 500 deg 2) consists of 3 narrow and disjoint 2.5° strips, which are less adequate for our analysis.

Our main sample, hereafter *SDSS all*, includes all objects classified as galaxies with extinction corrected magnitude $r < 21$, and a low associated error ($< 20\%$). This sample contains ~ 5 million galaxies distributed over the North sky. Its predicted redshift distribution is broad and has a median redshift $\bar{z} \sim 0.3$. Our high-redshift sample (*SDSS high-z* thereafter) comprises $\sim 3 \times 10^5$ galaxies, with $\bar{z} \sim 0.5$. It was selected by imposing magnitude cuts and color cuts perpendicular to the redshift evolution and the spectral type variations based on theoretical spectral synthesis models. We shall also compare our results to the APM analysis in Fosalba & Gaztañaga (2003), who used a $b_J = 17 - 20$ sample, $\bar{z} \simeq 0.15$, area ~ 4300 deg 2 and 1.2 million galaxies.

For the CMB data, we use the first-year full-sky WMAP maps (Bennett et al. 2003). Since the observed CMB-galaxy correlation is practically independent of the WMAP frequency band used (Fosalba & Gaztañaga 2003), we shall focus on the V-band (~ 61 GHz) as it conveniently combines low pixel noise and high spatial resolution, $21'$. In addition, we have also used the W-band and a foreground “cleaned” WMAP map (Tegmark et al. 2003) to check that our results are free from galactic contamination. We mask out pixels using the conservative Kp0 mask, that cuts out 21.4% of the sky (Bennett et al. 2003). All the maps used have been digitized into $7'$ pixels using HEALPix⁴, (Górski et al. 1999).

3. CROSS-CORRELATION AND STATISTICAL TESTS

We follow the notation introduced in Fosalba & Gaztañaga (2003). We define the cross-correlation function as the expectation value of density

¹ Institut d’Astrophysique de Paris, 98bis Bd Arago, 75014 Paris, France

² Institut d’Estudis Espacials de Catalunya/CSIC, Gran Capità 2-4, 08034 Barcelona, Spain

³ INAOE, Astrofísica, Tonantzintla, Puebla 7200, Mexico

⁴ <http://www.eso.org/science/healpix>

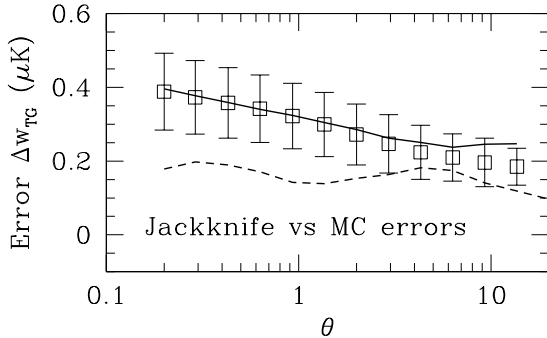


FIG. 1.— Errors in the cross-correlation $w_{TG}(\theta)$ from the dispersion in 200 Monte-Carlo simulations (solid line) as compared with the mean and dispersion (squares with errorbars) in the Jackknife (JK) error estimation over the same simulations. Dashed line correspond to the JK error in the real WMAP-SDSS *all* sample.

fluctuations $\delta_G = N_G / \langle N_G \rangle - 1$ and temperature anisotropies $\Delta_T = T - T_0$ (in μK) at two positions \hat{n}_1 and \hat{n}_2 in the sky: $w_{TG}(\theta) \equiv \langle \Delta_T(\hat{n}_1) \delta_G(\hat{n}_2) \rangle$, where $\theta = |\hat{n}_2 - \hat{n}_1|$.

We compute the CMB-galaxy correlation and the associated statistical error-bars using the jack-knife (JK) method described in (Fosalba & Gaztañaga 2003) and references therein. The survey is divided into $M = 16$ (we find similar results for $M = 8$) separate regions on the sky, each of equal area. The w_{TG} analysis is then performed M times, each time removing a different region, the so-called JK subsamples. The covariance C_{ij} for w_{TG} between scales θ_i and θ_j is obtained by re-scaling the covariance of the JK subsamples by a factor $M - 1$ (see Eq.[3] in Fosalba & Gaztañaga (2003)). To test the JK errors and covariance we have also run 200 WMAP V-band Monte-Carlo (MC) realizations. We add random realizations of the measured WMAP temperature angular power-spectrum (Bennett et al. 2003) to those of the white noise estimated for the relevant frequency band (Hinshaw et al. 2003). For each MC simulation we estimate the mean “accidental” correlation w_{TG} of simulated CMB maps to the SDSS galaxy density fluctuation map. We also estimate the associated JK error in each MC simulation. Fig.1 compares the ‘true’ sampling error from the dispersion of $w_{TG}(\theta)$ in 200 MC simulations with the mean and dispersion of the JK errors over the same simulations. The JK error gives an excellent estimate of the ‘true’ error up $\theta \simeq 5$ degrees. On larger scales it only underestimates the error by 10 – 20%, which is hardly significant given the uncertainties.

Fig.2 shows w_{TG} for the different samples together with the corresponding JK error. It turns out that the the JK errors from the real WMAP sample are in some cases smaller (up to a factor of two) than the JK errors (or sample to sample dispersion) from the MC simulations. Fig.1 shows, as a dashed-line, the comparison for the *SDSS all* sample, which exhibits the largest discrepancy. This difference in error estimation is not totally surprising as the MC simulations do not include any physical correlations and use a CMB power spectrum that is valid for the whole sky, and not constraint

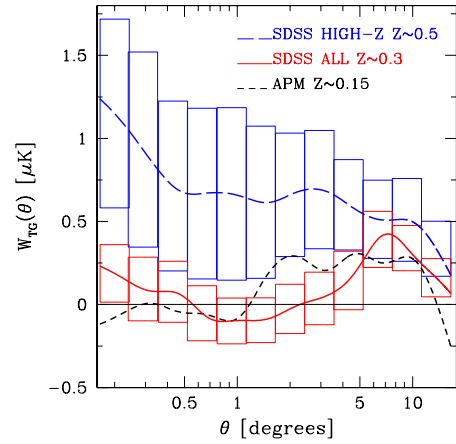


FIG. 2.— WMAP-SDSS correlation: long dashed-line shows the measurement for the *SDSS HIGH-Z* sample, while the solid line displays the correlation for the *SDSS ALL* sample. For reference, short-dashed line displays the same measurement using the APM galaxy survey instead of SDSS. Boxes show $1-\sigma$ error-bars.

as to match the CMB power over the SDSS region. The JK errors provide a model free estimation that is only subject to moderate (20%) uncertainty, while MC errors depend crucially on the model assumptions that go into the simulations. Despite these differences in the MC error estimation the overall significance for the detection turns out to be similar, as explained in §4.1.

We derive the significance of the detected correlation taking into account the large (JK) covariance between neighboring (logarithmic) angular bins in survey subsamples (but see also §4.1). Adjacent bins at large scales ($\theta > 4^\circ$) are correlated at the $\simeq 80\%$ level, dropping to $\simeq 40\%$ for alternative bins. Bins at smaller scales are progressively more correlated. To assign a conservative significance for the detection (ie against $w_{TG} = 0$) we estimate the minimum χ^2 fit for a constant w_{TG} and give the difference $\Delta\chi^2$ to the $w_{TG} = 0$ null detection. For example, at scales $\theta = 4 - 10^\circ$ we find: $w_{TG} = 0.53 \pm 0.21 \mu\text{K}$ for the *SDSS high-z* sample, $w_{TG} = 0.26 \pm 0.13 \mu\text{K}$ for the *SDSS all* sample and $w_{TG} = 0.35 \pm 0.13 \mu\text{K}$ for the APM, in all cases we give $1-\sigma$ errorbars.

We find the largest significance in the CMB-galaxy correlation for the *SDSS high-z* sample: $\Delta\chi^2 = 9.1$ (ie probability, $P = 0.3\%$ of no detection) for $\theta < 10^\circ$ (being $\chi^2_{min} = 14.6$ for $w_{TG} = 0.55 \mu\text{K}$ with 11 d.o.f., although the fit is only approximate as the signal drops with scale). In order to assess the significance levels for the ISW and SZ effects from the observed CMB-Galaxy correlations, we shall first introduce model predictions.

4. COMPARISON TO PREDICTIONS

The temperature of CMB photons is gravitationally redshifted as they travel through the time-evolving dark-matter gravitational potential wells along the line-of-sight, from the last scattering surface $z_s = 1089$ to us, $z = 0$ (Sachs & Wolfe 1967). At a given sky position \hat{n} : $\Delta T^{ISW}(\hat{n}) = -2 \int dz \Phi(\hat{n}, z)$, and for a flat universe $\nabla^2 \Phi = -4\pi G a^2 \rho_m \delta$ (see Eq.[7.14] in Peebles (1980)). In Fourier space it reads, $\Phi(k, z) =$

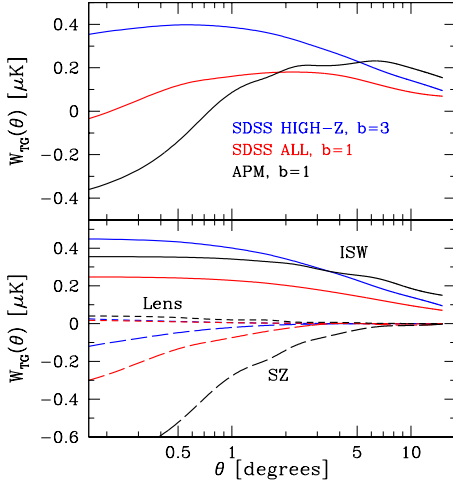


FIG. 3.— Theoretical predictions: (Bottom panel) Continuous, long and short dashed lines show the ISW, SZ and lensing predictions. Different sets of lines correspond to the APM (black), *SDSS all* (red) and *SDSS high-z* (blue) samples. (Top panel) The total prediction (ISW+SZ+Lensing) for the 3 samples. We have assumed a Λ CDM model with a fixed $b_{gas} = 2$ in all cases, $b = 3$ for *SDSS high-z* and $b = 1$ for APM and *SDSS all*.

$-3/2\Omega_m(H_0/k)^2\delta(k, z)/a$, and thus:

$$w_{TG}^{ISW}(\theta) = \langle \Delta_T^{ISW} \delta_G \rangle = \int \frac{dk}{k} P(k) g(k\theta) \quad (1)$$

being, $g(k\theta) = 1/2\pi \int dz W_{ISW}(z) W_G(z) j_0(k\theta r)$, where the ISW window is $W_{ISW} = -3\Omega_m(H_0/c)^2 \dot{F}(z)$, with $c/H_0 \simeq 3000h \text{ Mpc}^{-1}$, $\dot{F} = d(D/a)/dr = (H/c)D(f-1)$, and $f \simeq \Omega_m^{6/11}(z)$ quantifies the time evolution of the gravitational potential. The galaxy window function is $W_G \simeq b(z) D(z) \phi_G(z)$, which depends on the galaxy bias, linear dark-matter growth and the galaxy selection function. The ISW predictions for the 3 samples are shown in in bottom panel of Fig.3. Unless stated otherwise, we use the concordance Λ CDM model with $\Omega_m = 0.3$, $\Omega_\Lambda = 0.7$, $\Gamma \simeq h\Omega_m = 0.2$ and $\sigma_8 = 1$.

The weak lensing effect prediction is quite similar to the ISW, we just need to replace the time derivative of the Newtonian potential by its 2D Laplacian (Seljak & Zaldarriaga 1996): $W_{Lens} = 3k^2 \Omega_m(H_0/c)^2 (D/a)/d(r) d(r)$ being the angular distance to the lensing sources (with: $d(r_s - r)/d(r_s) \simeq 1$).

For the thermal Sunyaev-Zeldovich (SZ) effect, we assume that the gas pressure δ_{gas} fluctuations are traced by the galaxy fluctuations $\delta_{gas} \simeq b_{gas} \delta_G$ with a relative amplitude given by the gas bias, $b_{gas} \simeq 2$, representative of galaxy clusters, although b_{gas} is uncertain to within 50 % on linear scales and for low-z sources (Refregier & Teyssier 2002). A simple conservative estimate of the SZ effect is given by (Refregier et al. 2000):

$$w_{TG}^{SZ}(\theta) = -b_{gas} \overline{\Delta T} w_{GG}(\theta) \quad (2)$$

where $\overline{\Delta T}$ is the mean temperature change in CMB photons Compton scattered by electrons in hot intracluster gas. Following Refregier et al. (2000), we calculate $\overline{\Delta T} = j(x)\bar{y} T_0$, where $T_0 \simeq 2.73\text{K}$ is the mean CMB temperature, \bar{y} is the mean Compton parameter induced by galaxy clusters, and $j(x) = -4.94$ is the negative SZ

spectral factor for the V-band. The Compton parameter can be calculated integrating along the line of sight the normalized galaxy redshift distribution convolved with the volume-averaged density-weighted temperature. The latter is obtained from the mass function and the M-T relation. We assume the Seth & Tormen mass function (Sheth & Tormen 1999; Sheth et al. 2001) and the M-T relation given by Borgani et al. (1999). In summary, we obtain for the WMAP V-band, $\overline{\Delta T} = 6.65\mu\text{K}$ for the *SDSS all* sample, and $\overline{\Delta T} = 6.71\mu\text{K}$ for the *SDSS high-z* sample which corresponds to $\bar{y} \simeq 1.35 \times 10^{-6}$ for both samples. The SZ predictions for the 3 samples are shown in the bottom panel of Fig.3. Note the galaxy auto-correlation explains most of the differences observed.

The total predicted correlation is thus the sum of three terms: the ISW, thermal SZ and Lensing contributions, $w_{TG} = w_{TG}^{ISW} + w_{TG}^{SZ} + w_{TG}^{Lens}$. Fig.3 shows individual contributions of these effects (bottom panel) and the total (top) for the 3 samples analyzed. The ISW effect typically dominates for angles $\theta > 4^\circ$, while the SZ effect is expected to be significant on small scales $\theta < 1^\circ$. Lensing is found to be negligible at all scales for our samples.

Before we can make a direct comparison between theory and observations, we shall address the issue of galaxy bias. The higher redshift sample requires a high bias $b > 1$ to explain the large cross-correlation seen at all scales (the SZ effect being smaller at high redshift). At low redshifts the measured correlation is dominated by the thermal SZ on small scales ($\theta < 1^\circ$) and by ISW on large-scales ($\theta > 4^\circ$). Here no bias is required to match the observations. This agrees quite well with our self-consistent bias estimation: for each sample we can estimate the ratio $b^2 \simeq w_{GG}/w_{MM}$, where w_{MM} and w_{GG} are the (theoretically predicted) matter and (measured) galaxy auto-correlation functions. For APM and *SDSS all* samples we find $b^2 \simeq 1$, while for the *SDSS high-z* sample we get $b^2 \simeq 6$.

4.1. Significance tests

ISW effect: On large scales $\theta > 4^\circ$, the ISW effect is expected to dominate for all survey depths (see Fig 3). Therefore, from the large-angle CMB-Galaxy correlation, we can directly infer the ISW effect (ie, $w_{TG} = w_{TG}^{ISW}$, see end of §3). In particular, for the *SDSS high-z* sample, a constant correlation fit rejects the null detection with high significance $\Delta\chi^2 = 6.0$ ($P = 1.4\%$), comparable to the level found for the APM survey, $\Delta\chi^2 = 6.1$ ($P = 1.3\%$). A smaller significance is obtained for the *SDSS all* sample: $\Delta\chi^2 = 3.9$ ($P = 4.8\%$). Alternatively, we can use the uncorrelated MC simulations (see §3) to have an independent estimate of the significance. When a particular MC simulation has an accidentally large value of w_{TG} it also has a large JK error associated. We can thus assign a significance to our measurement by asking how many of the 200 MC simulations have a value of w_{TG} equal or larger than the observations with an associated JK error equal or smaller than found for the observations. We find that only two of the MC simulations fulfil this condition in any of the samples, meaning that the significance of each detection is better than 1% (for each of the 3 different data samples).

Since these samples are basically independent, we can combine them to infer a total significance for the ISW

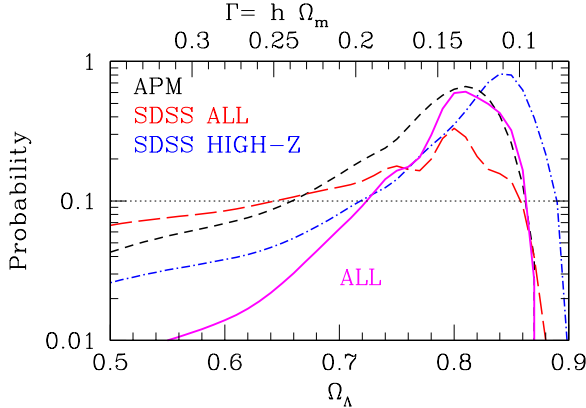


FIG. 4.— Estimating dark-energy: Long-dashed, short-dashed and dot-dashed lines show the probability distribution for Ω_Λ in the *SDSS all*, APM and *SDSS high-z* samples. The combined distribution (for 3 d.o.f.) is shown by the solid line.

detection: we find a total $\Delta\chi^2 = 16$ ($P = 0.1\%$ for 3 d.o.f) corresponding to a 3.3σ . Note we could do better using a (scale dependent) Λ CDM model theory prediction, but at the cost of introducing model dependent detection levels. Moreover, we can further include the ISW-dominated small angle bins in our deepest sample, where SZ is negligible, increasing the significance to $\Delta\chi^2 = 18.8$, ($P = 0.03\%$ for 3 d.o.f.), ie we detect the ISW effect at the a 3.6σ level.

SZ effect: We can estimate the significance of the drop in the signal at small angles in the *SDSS all* and APM samples due to the SZ effect (see Fig3) using the best-fit constant at large angles (ie, the ISW signal) and ask for the observed deviation from such value at smaller scales. For $\theta < 1^\circ$, we find: $w_{TG}^{SZ} = -0.27 \pm 0.11$ for *SDSS all*, and $w_{TG}^{SZ} = -0.41 \pm 0.16$ for APM (1- σ errorbars). Note this is conservative because the ISW increases slightly as we approach smaller scales (see §IV). This test gives $\Delta\chi^2 = 5.5$ ($P = 2\%$) for the *SDSS all* sample and $\Delta\chi^2 = 8.5$ ($P = 0.3\%$) for the APM.

5. DISCUSSION

We have measured the CMB-galaxy correlation using WMAP and the SDSS DR1 galaxy survey. We measure

a significant cross-correlation at low ($z \sim 0.3$) and high ($z \sim 0.5$) redshifts. We detect a positive correlation on large-scales induced by the ISW effect at the 2σ level for the (broadly distributed) low- z sample. This correlation is similar to that measured for the lower redshift ($z \sim 0.15$) APM galaxies (Fosalba & Gaztañaga 2003), although the latter has a larger significance, 2.5σ . Moreover, the significance of the detection raises to 3σ for the SDSS high- z sample. The combined analysis for the 3 samples gives a 3.6σ significance (see §4.1).

Our measurements at large scales are in good agreement with ISW predictions for a dark-energy dominated universe. Fig 4 shows the probability distribution for Ω_Λ in a flat Λ CDM model. We have fixed $\sigma_8 = 1$, $h = 0.7$ and $\Omega_M + \Omega_\Lambda = 1$. As we vary Ω_Λ the shape parameter for the linear power spectrum $P(k)$ consistently changes $\Gamma = h\Omega_M$ (Bond & Efstathiou 1984). We only use the data for $\theta > 4^\circ$, where the ISW is the dominant contribution. We fix the bias b by comparing the matter angular auto-correlation function in each model to the galaxy auto-correlation in each sample. We find $b \simeq 1$ for the APM and *SDSS all* samples and $b \simeq \sqrt{6}$ for the *SDSS high-z* sample. The $\Delta\chi^2$ value in each model refers to the minimum χ^2 fit to a constant in the range $4^\circ < \theta < 10^\circ$. As can be seen in the figure, all samples prefer large values of Ω_Λ , with the best fit $\Omega_\Lambda \simeq 0.8$ with a 2σ range $\Omega_\Lambda = 0.69 - 0.87$.

We also see evidence (2.7σ level) for the thermal SZ effect from the drop of the CMB-galaxy correlation on small-scales in the low- z samples of SDSS and APM galaxies. These new measurements can be used to constrain the redshift evolution of the physical properties of gas inside galaxy clusters.

PF wants to thank Francois Bouchet for useful suggestions. FJC acknowledges useful discussions with Andy Connolly. We acknowledge support from the Barcelona-Paris bilateral project (Picasso Programme). PF acknowledges a post-doctoral CMBNet fellowship from the EC. EG and FJC acknowledge the Spanish MCyT, project AYA2002-00850, EC-FEDER funding.

REFERENCES

- Abazajian K., et al. 2003, AJ, submitted, astro-ph/0305492
- Baugh C. M., Gaztañaga E., 1996, MNRAS, 280, 37
- Bennett, C. L., et al. 2003, ApJ, submitted, astro-ph/0302207
- Bond, J.R., Efstathiou, G. 1984, ApJ, 285, 45
- Borgani, S., et al. 1999, ApJ, 517, 40
- Boughn, S. P. & Crittenden, R. G. 2003, astro-ph/0305001
- Fosalba, P., & Gaztañaga, E., 2003, astro-ph/0305468
- Górski, K. M., Hivon, E., & Wandelt, B. D. 1999, in Evolution of Large-Scale Structure: From Recombination to Garching
- Hernandez-Monteagudo, C. & Rubino-Martinez, J.A., 2003, astro-ph/0305606
- Hinshaw, G. F. et al. 2003, astro-ph/0302222
- Maddox, S. J., et al. 1990, MNRAS, 242, 43
- Myers, A.D., et al. 2003, astro-ph/0306180
- Nolta M.R., et al. 2003, astro-ph/0305097
- Peebles, P. J. E. 1980, The Large-Scale Structure of the Universe (Princeton, NJ: Princeton University Press)
- Refregier, A., Spergel D. N., Herbig T., 2000, ApJ, 531, 31
- Refregier, A., Teyssier, R., 2002, PRD, 66, 43002
- Sachs, R. K. & Wolfe, A. M. 1967, ApJ, 147, 73
- Scranton, R., et al. 2003, astro-ph/0307335
- Seljak, U. & Zaldarriaga, M. 1996, ApJ, 538, 57
- Sheth, R. K. & Tormen, G. 1999, MNRAS, 308, 119
- Sheth, R. K., Mo, H. J. & Tormen, G. 2001, MNRAS, 323, 1
- Tegmark, M., et al. 2003, astro-ph/0302496
- York, D. G., et al. 2000, AJ, 120, 1579